Eng. Research Bull.
Faculty of Eng. & Tech.
Menoufia University
Vol. VI Part 1,1984

pp. 215 - 235

TORQUE/SPEED CONTROL OF INDUCTION MOTORS USING A D.C. CHOPPER CIRCUIT

S.A.MAHMOUD , A.E.LASHIN and S.A.HASSAN
TEam of Control of Electrical Machines (TECEM)
Faculty of Eng. & Tech., Menoufia University,
Shebin El-Kom, Egypt.

ABSTRACT

In this paper the torque and speed of an induction motor is controlled using a chopper circuit on the rotor side. An experimental control system is built and tested. Detail design of the chopper control circuit and the circuits associated with the control system are reported.

It is shown that the torque can be kept constant over a wide speed range. Simplified models are used ; the torque-slip characteristics and the harmonic content in the a.c. component of the rectified current are predicted and compared with test results. It is also shown that dynamic braking can be performed using the rectified rotor current.

A closed loop control of the motor speed is also performed. Calculations have been carried out in order to predict suitable system parameters for acceptable response. The control system stabilizes the speed against load torque variations using a proportional-plus-integral controller. Computed response is compared with results obtained experimentally.

LIST OF SYMBOLS

F	Friction coefficient.
k	$= I_{max}/I_{min}$.
n	Number of operating cycle.
I_d, I_{rms}	Average and rms value of the rectified rotor current, respectively.
I_{op}, I_{sh}	Steady-state rectified current when the chopper is "OFF" and "ON" all the time, respectively.
J	Moment of inertia for the motor with its load.
R_1	Resistance of external inductor.
R_{eq}	Effective resistance of chopper-controlled resistance.
R_{sh}	Current sensing resistance.
r_1, r_2	Stator and rotor resistance, respectively.
T	Developed torque.
T_{ch}	Chopper period.
x_1, x_2	Stator and rotor reactance, respectively.
x_1', x_2'	Stator and rotor reactance referred to rotor, respectively.
x_m	Stator magnetizing reactance.
ω_s	Synchronous speed.
β	Duty cycle of the chopper circuit.

1. *INTRODUCTION*

With the recent advancement in power semiconductor technology, induction motors are being widely used in variable speed industrial drives. The speed of an induction motor is determined by the supply frequency and rotor slip. In practice, the slip of an induction motor, and accordingly its speed, can be controlled by drawing electrical power from the rotor circuit. Conventional methods employ variable resistances in the rotor circuit which imply energy loss. With the advent of power semiconductor devices a stepless rotor resistance control can be done using a chopper switch [1,2]. The chopper is a

power switch electronically monitored by a control circuit, which varies the effective rotor resistance as designed in stepless and contactless manner. It can be used to control the torque/current and to achieve an improved power factor. It can also be used with closed loop speed and current controllers [3,4].

In this paper a chopper circuit is built and tested. The Schmitt trigger control is used to build a control and firing circuit [5]. The system performance at constant torque operation is studied. Also the experimental and calculated results of the torque control operation are compared.

A closed loop speed control, with a proportional-integral (PI) controller is built and tested. The dynamic performance of the closed loop system is also studied and compared with the experimental results.

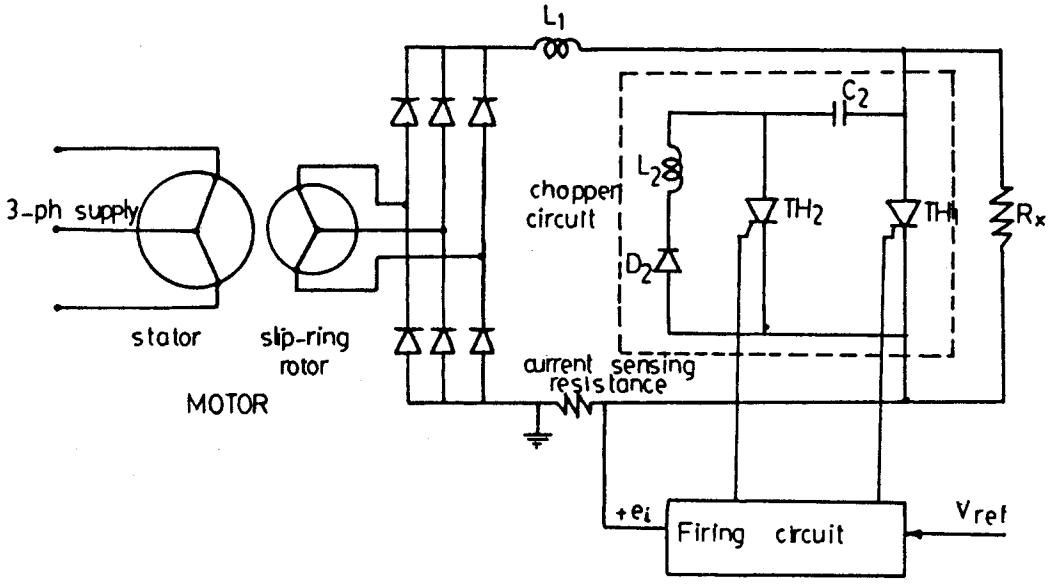

Fig.(1) Power circuit for constant current operation.

2. PRINCIPLE OF ROTOR RESISTANCE CONTROL

The system under consideration is shown in Figure(1). The rotor power is rectified by a three-phase diode-bridge. A smoothing inductor L_1 and an additional resistor R_x are connected in series across the diode bridge. A chopper switch is used across the resistor R_x to perform control of the rotor current, e.g. to switch R_x in and out of the rotor circuit.

When the chopper is "ON" the additional resistance in the rotor circuit is nearly zero, and the rectified rotor current rises to its maximum level I_{max}. When the chopper is "OFF" the additional resistance in the rotor circuit is R_x, and the rectified rotor current drops to its minimum level I_{min}; this mechanism is shown in Figure (2). According to the desirable average rotor current, the two limits I_{max} and I_{min} are set in the firing and control circuits to determine the ON and OFF periods of the thyristor chopper.

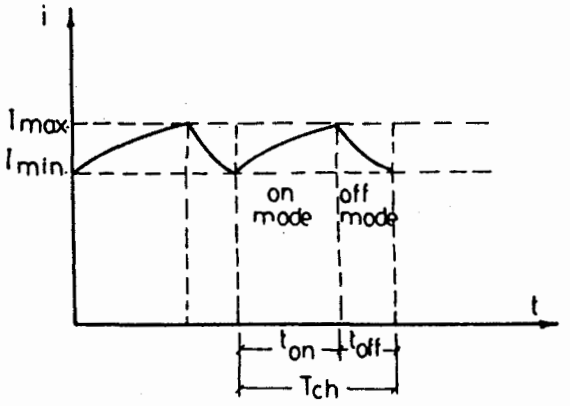

Fig.(2) The waveshape for current limit control.

A voltage proportional to the rectified current is used as a control signal to the firing circuit. The control circuit must be capable of supplying a firing pulse to the main thyristor TH_1 when the rectified current reaches the required minimum level, I_{min}. It should be also supply a pulse to the auxiliary thyristor TH_2 when the current reaches the maximum level, I_{max}. In order to

perform the above requirements, the Schmitt trigger circuit is employed.

The control circuit logic is shown in Figure (3). It consists of the Schmitt trigger circuit, differentiator, and pulse amplifier. Those are described in Appendix A.

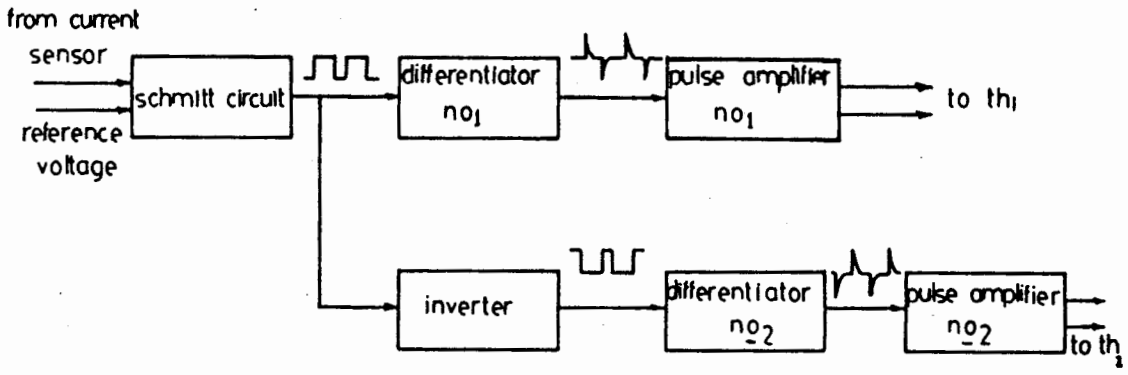

Fig.(3) Firing circuit logic

3. *MATHEMATICAL ANALYSIS*

In the system under consideration the rotor circuit resistance of the motor is subjected to a modulation process and so it may be difficult to follow an exact methods for analysis. The rotor resistance modulation and the rectifier effect cause distortion of the motor currents. Accordingly, development of an exact model considering the above effects may not be possible. Since, the rectifier-chopper circuitry adds nonlinearities into the equations of the system. A simplified model for the system is developed using the conventional per phase equivalent circuit and a satisfactory results have been obtained.

The system can be represented using the motor model referred to the d.c. side and the following simplifying assumptions are made :

1] The stator power loss is neglected.

2] The voltage drop across stator impedance is neglected, e.g. $E_1 = V_1$, but the effect of the stator leakage inductance on rectifier operation is considered.

3] The rectified current is considered smooth. Accordingly, the rotor current is a rectangular wave of $\frac{2\pi}{3}$ duration.

The rotor rms current, I_2, is thus given by [6] :

$$I_2 = \sqrt{\frac{2}{3}}\ I_d \qquad (1)$$

The power loss in the rotor resistance for all three phase is

$$P_{r\ loss} = 3\ I_2^2\ r_2 = 2\ I_d^2\ r_2 \qquad (2)$$

Then, the rotor resistance is represented by $(2\ r_2)$ in the d.c. side for the three-phase system.

From the conventional theory of rectifiers, it is known that presence of reactances on the a.c. side of the bridge cause current overlap during change over (i.e., commutation) of conducting diodes. This results in loss of voltage during commutation period, and its average effect over a cycle is to produce an equivalent d.c. voltage drop given by [6] :

$$V_{c\ell} = \frac{3}{\pi}\ S(x_1' + x_2)\ I_d \qquad (3)$$

Hence, as far as the effect of overlap on the rectified voltage is concerned the term $\frac{3}{\pi}\ (x_1' + x_2)$ can be treated as a resistance and so Equation (3) becomes

$$V_{c\ell} = S\ R_m\ I_d$$

Then, the equivalent circuit of the motor referred to the d.c. side is set as shown in Figure (4), the output voltage of rectifier bridge at standstill is given by ; $E_{do} = \frac{3\sqrt{6}}{\pi}\ E_1'$ and at slip S, the output voltage becomes $E_{dc} = S\ E_{do}$. The developed torque at slip S is therefore expressed as

$$T = \frac{P_{cu}}{S\omega_s} = (E_{do}\ I_d - R_m\ I_d^2)/\omega_s \qquad (4)$$

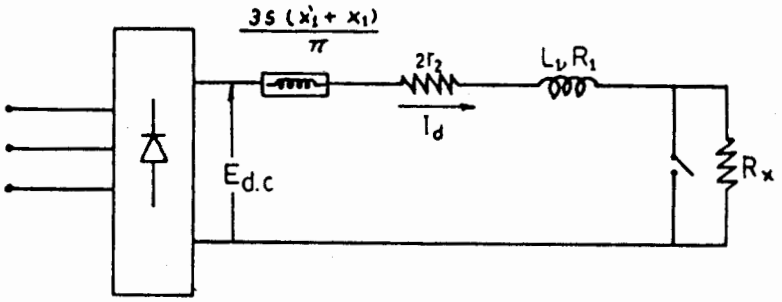

Fig.(4) Motor equivalent circuit referred to d.c. side.

3.1. Modes of Operation

Considering Figure (2), two modes of the circuit operation are studied. Those are as follows :

a- The "ON" Mode : $n\,T_{ch} \leq t \leq (n+\beta)\,T_{ch}$

At the instant $t = nT_{ch}$, the rectified current $i_d = I_{min}$ and the main thyristor is turned to the "ON" state. The waveshape of the d.c. current can be predicted as follows :

From the circuit model

$$E_{dc} = (SR_m + 2r_2 + R_1)\, i_d + L_1 \frac{di_d}{dt}$$

The solution for $i_d(t) = i_{on}(t)$ is thus

$$i_{on}(t) = I_{sh} + (I_{min} - I_{sh}) Exp[-(t-nT_{ch})/\tau_{on}] \qquad (5)$$

where

$$\tau_{on} = \frac{L_1}{SR_m + 2r_2 + R_1} \quad \text{and} \quad I_{sh} = \frac{E_{dc}}{SR_m + 2r_2 + R_1}$$

b- The "OFF" Mode : $(n+\beta)T_{ch} \leq t \leq (n+1)T_{ch}$

At the instant $t = (n+\beta)\,T_{ch}$, the rectified current $i_d = I_{max}$ and the main thyristor is turned to the "OFF" state. The rectified current can be predicted as follows:

$$E_{dc} = (SR_m + 2r_2 + R_1 + R_x)\, i_d + L_1 \frac{di_d}{dt}$$

The solution for $i_d(t) = i_{off}(t)$ is thus

$$i_{off}(t) = I_{op} + (I_{max} - I_{op})\, Exp\,[-\{t-(n+\beta)T_{ch}\}/\tau_{off}] \qquad (6)$$

where

$$\tau_{off} = \frac{L_1}{SR_m + 2r_2 + R_1 + R_x} \quad \text{and} \quad I_{op} = \frac{E_{dc}}{SR_m + 2r_2 + R_1 + R_x}$$

3.2. *Minimum External Resistance and Critical Slip*

During steady-state operation the system control operates such that, the levels for currents must be satisfied, e.g.

$$i_{on}\ ((n+\beta)T_{ch}) = i_{off}((n+\beta)T_{ch}) \tag{7}$$

and

$$i_{on}\ (n\ T_{ch}) = i_{off}((n+1)T_{ch}) \tag{8}$$

From Equations (5) and (7), the upper current limit can be obtained as :

$$I_{max} = I_{sh} + (I_{min}-I_{sh})\,Exp(-\beta T_{ch}/\tau_{on}) \tag{9}$$

From Equations (6) and (8), the lower limit is obtained as :

$$I_{min} = I_{op} + (I_{max}-I_{op})\,Exp[-(1-\beta)T_{ch}/\tau_{off}] \tag{10}$$

From Equations (9) and (10), the chopping period is obtained as :

$$T_{ch} = -[\tau_{on}\ell n(\frac{I_{sh}-I_{max}}{I_{sh}-I_{min}}) + \tau_{off}\ell n(\frac{I_{min}-I_{op}}{I_{max}-I_{op}})] \tag{11}$$

The critical slip S_{cr} for a given I_{max}, is determined by

$$S_{cr} = \frac{I_{max}(2\ r_2+R_1)}{E_{do}-I_{max}(R_m)} \tag{12}$$

The minimum value of the external resistance, for a given I_{min}, is given by equating I_{op} to I_{min} at standstill, where the rectified rotor voltage is at its maximum[5]. Then

$$(R_{ex})_{min} = \frac{E_{do}}{I_{min}} - (2\ r_2 + R_m + R_1) \tag{13}$$

4. *SYSTEM PERFORMANCE*

To obtain the system performance a computer program to calculate the system equations has been developed for the following :

4.1. Constant Torque Operation

A direct control of torque can be used to achieve rapid acceleration and retardation such as in cranes and traction system.

Using Equation (4) with $I_d = I_{sh}$, the torque-slip characteristic for different levels of I_{max} to I_{min} can be obtained as shown in Figure (5). From which it is obvious that, the spike in the characteristics decreases as the ratio k is decreased. This is due to the fact that, the chopper stays "ON" all the time for speed higher than the critical speed.

Also the experimental results were obtained at I_{min} = 5.75 A and K = 1.29. Figure 5, indicates also the experimental torque-slip characteristic, where close agreement between computed and test results is achieved. Figures 6.a, b and c show oscillograms for the rectifier, rotor and stator currents. The third oscillograms indicate that, the effect of the chopper controller on the stator current waveform is small. The machine parameters and other necessary data are provided in Appendix (B).

4.2. Ripple Factor

The current ripple factor is defined as

$$C.R.F. = \sqrt{C.F.F. - 1}$$

Where C.F.F. is the current form factor = I_{rms}/I_d, and from Equations (5) and (6), I_{rms} and I_d can be obtained. Figure (7) shows variation of the rectified current ripple factor with slip at different values of K. It is shown that the current ripple factor decreases as this ratio is decreased.

4.3. Harmonic Content

The Fourier algorithm [5] is used with Equations (5) and (6). The harmonic content in the a.c. component of the rectified current is obtained. Figures 8.a and b show

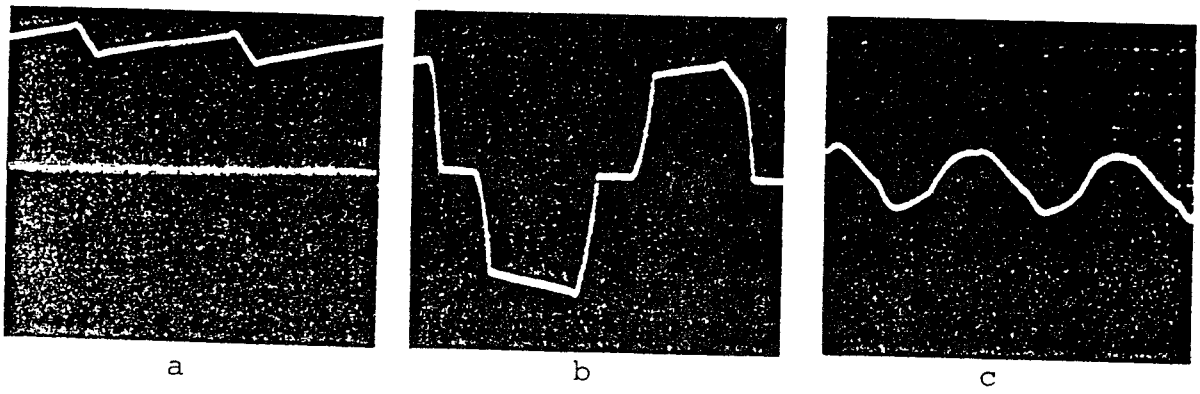

Fig.6. Oscillograms for (a) Rectified current. (b) Rotor current. (c) Stator current.

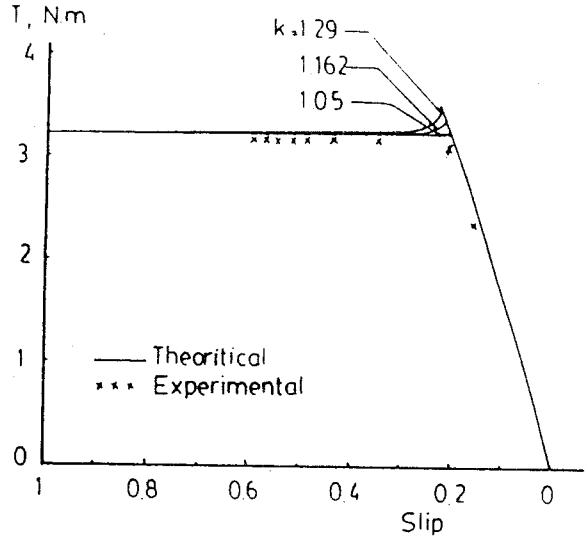

Fig.(5) Torque-slip characteristics

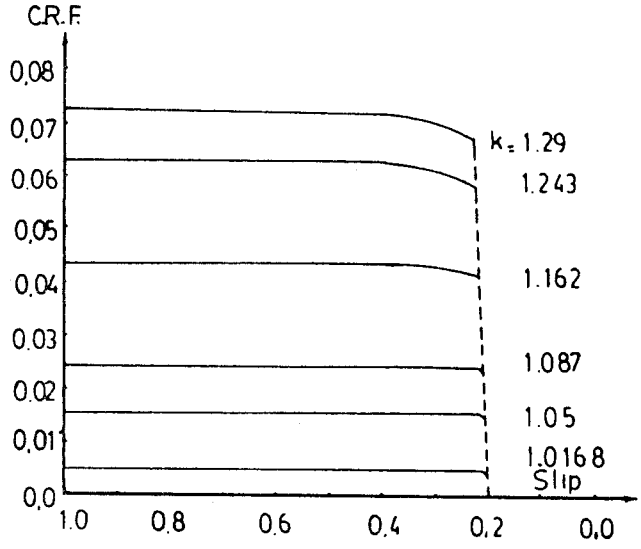

Fig.(7) Rectified current ripple factor with slip.

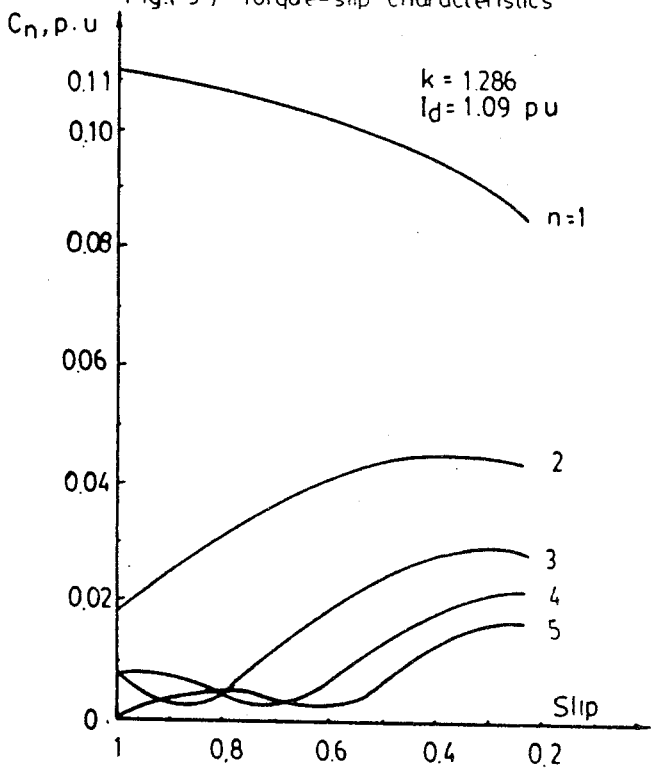

Fig.(8-a) Harmonics-slip relationship for k=1286

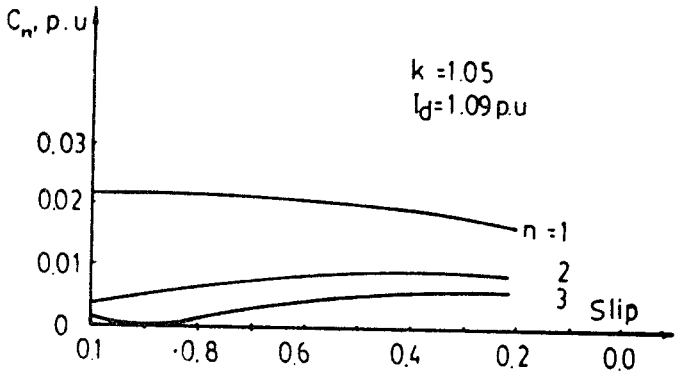

Fig.(8-b) Harmonics slip relationship for k=1.05

variations of the relative amplitude of harmonics with slip for different values of K, and the average rectified current, I_d, is constant, from which, levels of different harmonic components are decreased as K is decreased.

4.4. Dynamic Braking :

If the induction motor terminals are disconnected from the supply, the motor will come to rest under natural braking, and the braking time will be large as shown in Figure (9) (braking time ≅ 5.7 sec.). For faster braking, the motor terminals are disconnected from the a.c. supply and connected to a d.c. source. The machine operates as a generator, and part of kinetic energy of the rotating system is converted to electrical energy and dissipated in the rotor circuit. The braking time as a function of d.c. current excitation to the stator windings is shown in Figure (10). If the rectified rotor power is fed to the stator windings, no separate d.c. source is required for the braking operation. Therefore, a capacitor, C_1 = 100 μF, and a diode, D_1, are used across the diode bridge to hold the voltage for stator excitation immediately after the stator terminals are disconnected from the a.c. supply. The proposed circuit is shown in Figure (11-a). Figure (11-b) shows that, the motor experiences a hard brake and comes to rest at 1.1 sec., compared with the natural braking at the same condition which lasts 5.7 sec (Figure 9). Thus faster braking is obtained using the proposed arrangement.

5. SPEED CONTROL

With open loop control, the motor has very poor speed regulation. However, in many industrial applications, speed regulation of the drive is essential. In such cases it becomes necessary to employ closed-loop speed control.

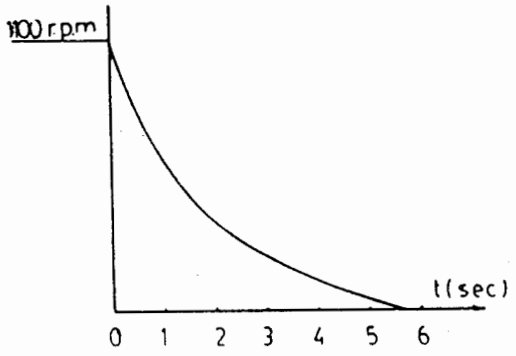

Fig.(9) The motor natural braking

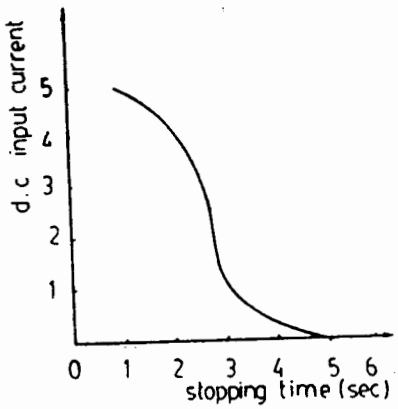

Fig.(10) Stopping time as function of d.c dynamic braking current.

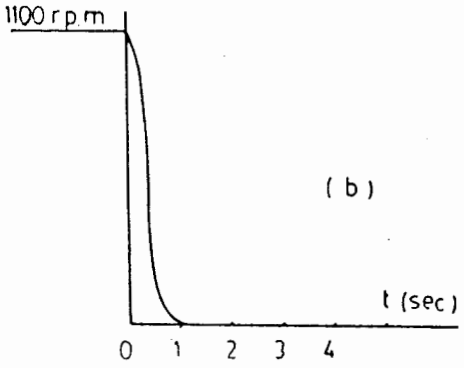

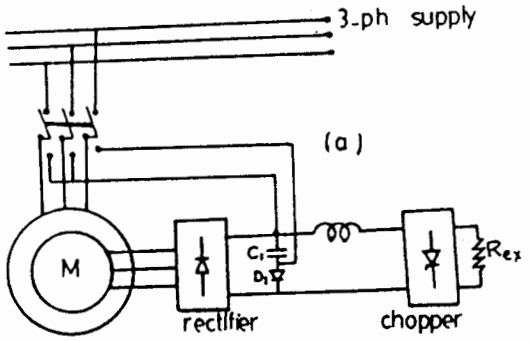

Fig.(11) Stator excitation fed from rotor circuit for d.c dynamic braking
(a) Basic circuit (b) Hard braking using this scheme

For closed loop operation, a tachogenerator mounted on the motor shaft is used to obtain a speed feedback signal (Figure 12). Also, the rotor current is sensed, using a small resistance on the d.c. side of the rectifier. The voltage signal (e_3) (the output of the current sensing resistance) is used to control the switching frequency of the chopper circuit. The duty cycle of the chopper circuit is varied with (e_2), that is the output of the speed controller. A simple arrangement of proportional-integral speed controller is used for giving improved speed regulation. The complete block diagram of the system is shown in Figure (13).

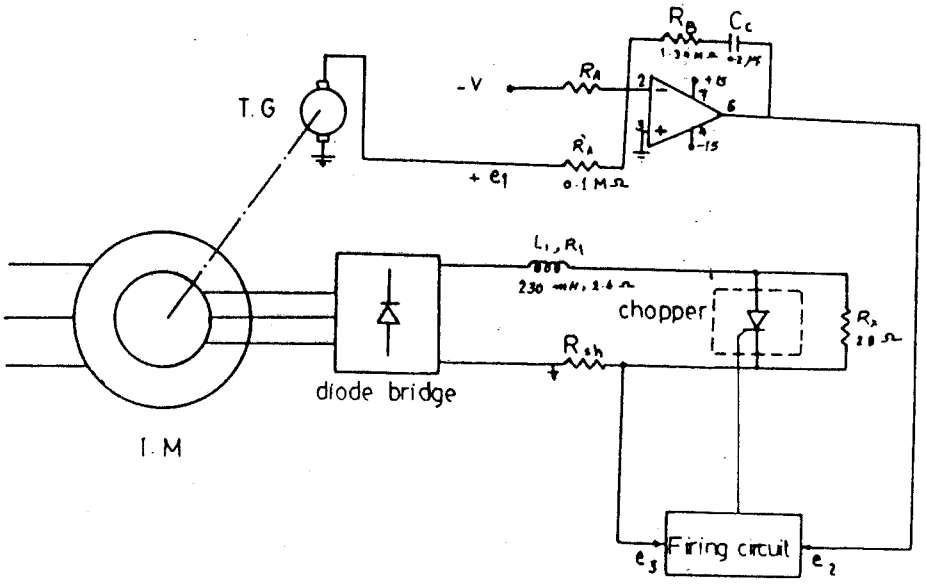

Fig.(12) The complete circuit for closed loop speed control

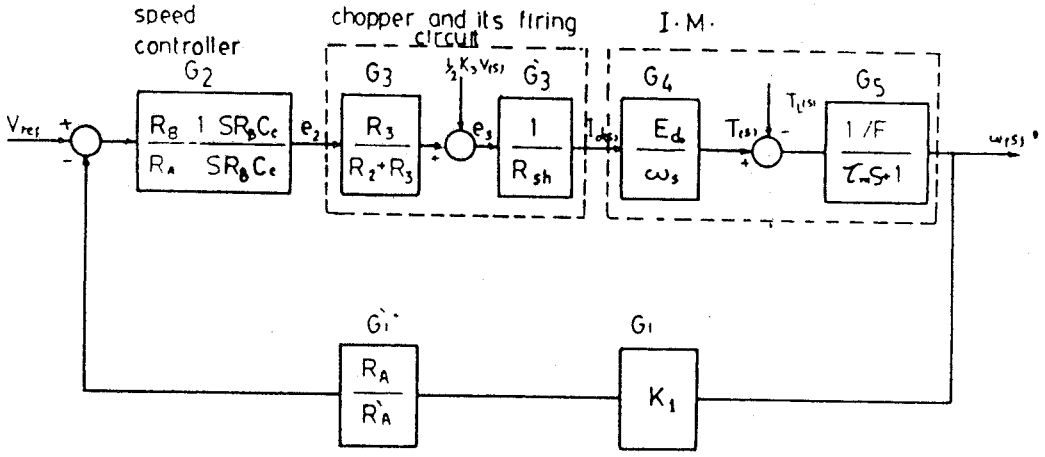

Fig.(13) The complete Block Diagram of the system

5.1. *Transfer Functions*

To study the transient response of the closed-loop system around the given operating point, the transfer function of each part of the system is developed as follows :

5.1.1. *Motor and its load*

Using Equation (4), with neglecting the voltage drop due to commutation, the torque developed by the motor becomes

$$T(s) = \frac{E_{do}}{\omega_s} I_d(s)$$

and

$$G_4(s) = T(s)/I_d(s) = E_{do}/\omega_s \qquad (14)$$

The transfer function of the mechanical system can be written as :

$$G_5(s) = \frac{\omega(s)}{T(s)-T_L(s)} = \frac{1/F}{1+S\ \tau_m} \qquad (15)$$

where

$\tau_m = J/F$ is the mechanical time constant.

5.1.2. *Chopper and its control circuit*

To develope the transfer function of the chopper and its control circuit, the following simplifying assumptions are used :

a- The chopper switching frequency is much greater than that of the rotor circuit ($f_{ch} >> f_r$)

b- $I_d \cong (I_{max} + I_{min})/2$

With the above assumptions, the response due to Schmitt trigger and triggering equipment as well as chopper response are obtained in approximately zero time (see Appendix A).

$$e_3 = (V_1 + V_2)/2 \qquad (16)$$

and

$$e_3(s) = G_3(s)\ e_2(s) + \tfrac{1}{2}\ K_3\ V(s) \qquad (17)$$

where $K_3 = K_3/(R_1+R_3)$, $G_3(s) = R_3/(R_2+R_3)$ and $G_3(s) = \frac{1}{R_{sh}}$

5.1.3. *Tachogenerator and its filter*

The overall transfer function of the tachogenerator and its associated filter could be written as

$$\frac{e_1(s)}{\omega(s)} = G_1(s) = \frac{K_1}{1 + ST_1} \qquad (18)$$

K_1 is the combined gain of the tachogenerator/filter combination, and T_1 is the time constant. This time constant is very small and so it can be neglected. Thus

$$G_1(s) \cong K_1 \qquad (19)$$

5.1.4. *Speed controller*

P.I controller was used to eliminate the steady-state error in the system response. The transfer function of the controller is given as :

$$G_2(s) = \frac{K_1(1 + S\,T_2)}{S\,T_1} \qquad (20)$$

5.2. *System Response*

From Figure (13), it can be shown that, the system is a second order. The characteristic equation of the system is given by :

$$S^2 + \frac{1}{\tau_m}\left(1 + \frac{R_B}{R'_A} K'_1\right) S + \frac{1}{\tau_m} \frac{1}{C_c R'_A} K'_1 = 0 \qquad (21)$$

where

$$K'_1 = k_i \cdot \frac{1}{F} \cdot \frac{E_{do}}{\omega_s} \cdot \frac{R_3}{R_{sh}(R_2+R_3)}$$

Equation (21) is used to predict the controller parameters, C_c and R_B.

Hence,

$$2\delta\omega_n = \frac{1}{\tau_m}\left(1 + \frac{R_B}{R'_A} k'_1\right) \text{and } \omega_n = \sqrt{\frac{1}{\tau_m} \frac{1}{C_c R'_A} k'_1}$$

The response of speed to a step change in V_{ref} and/or T_L is

$$\omega(t) = A_1 + A_2 e^{-\delta\omega_n t} \cos \omega_d t + \frac{A_3 - \delta\omega_n A_2}{\omega_d} e^{-\delta\omega_n t} \sin \omega_d t \quad \ldots(22)$$

where

$$A_1 = \frac{R'_A}{R_A K_1} V_{ref}, \quad A_2 = -\frac{R'_A}{R_A K_1} V_{ref}, \quad A_3 = -\frac{R'_A}{R_A K_1 \tau_m} V_{ref} - \frac{T_L}{\tau_m F}$$

and $\omega_d = \sqrt{\omega_n^2 - (\delta\omega_n)^2}$

Also, the response in the rectified current, I_d, due to a step change in V_{ref} and/or T_L is obtained from :

$$I_d(t) = B_1 + B_2 e^{-\delta\omega_n t} \cos \omega_d t + \left(\frac{B_3 - \delta\omega_n B_2}{\omega_d}\right) e^{-\delta\omega_n t} \sin \omega_d t \quad (23)$$

where

$$B_1 = \left(\frac{R'_A F}{R_A K_1} V_{ref} + T_L\right) \frac{\omega_s}{E_{do}}, \quad B_2 = \left[\left(\frac{K'_1 F R_B}{K_1 R_A} - \frac{R'_A F}{R_A K_1}\right) V_{ref} - T_L\right] \frac{\omega_s}{E_{do}}$$

and $$B_3 = \left[\left(\frac{K'_1 F}{K_1 R_A C_c} - \frac{R'_A F}{R_A K_1 \tau_m}\right) V_{ref} - \frac{T_L}{\tau_m}\right] \frac{\omega_s}{E_{do}}$$

The parameters of the closed loop system are given in Appendix B.

5.3. Results

The calculated results of speed and current response for a step change in V_{ref} are shown in Figure (14). The oscillograms of speed and current response are shown in Figure (15). Second-order response, and good damping assumed in the design procedure are obvious. Figure (16) shows the calculated speed and current response for a step change in T_L. The oscillograms of these responses are shown in Figure (17). The speed returns back to its initial value in about 1 sec. and the difference between I_{max} and I_{min} is constant for different levels of the average rectified current.

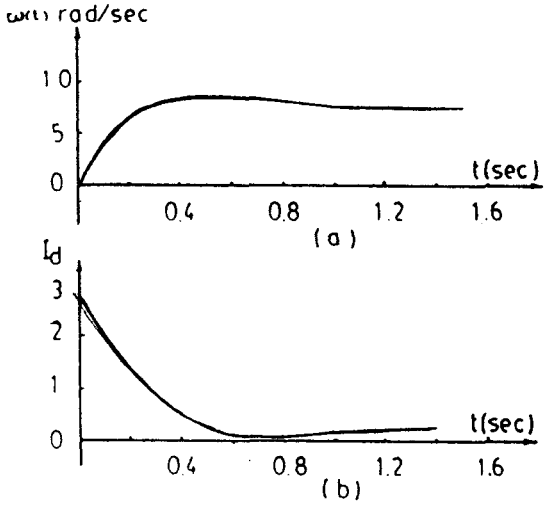

Fig. (14) Response of a step change in V_{ref}
(a) Speed Response
(b) Current Response

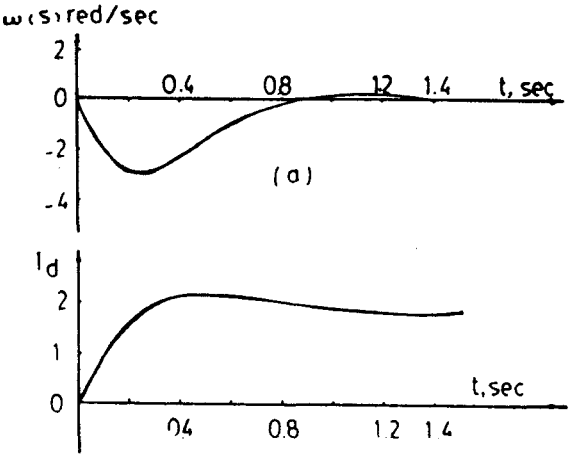

Fig. (16) Response for a step change in T_L
(a) Speed Response
(b) Current Response

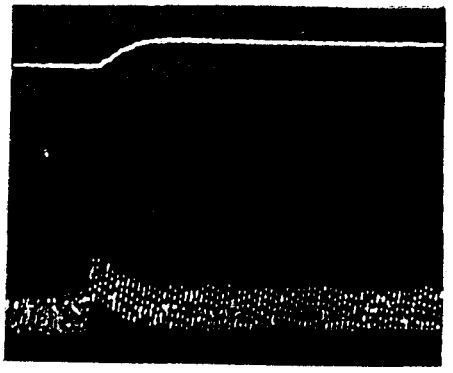

Fig. (15) The Oscillograms of speed Response. and current Response for a step change in V_{ref}.

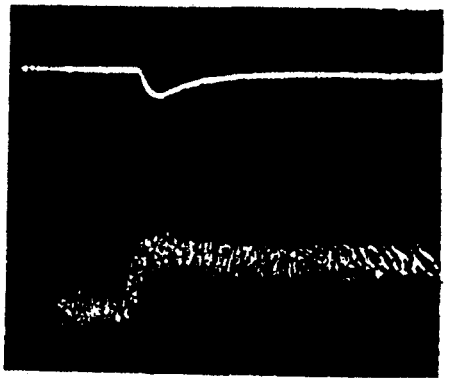

Fig. (17) The Oscillograms of speed response and current response for a step change in T_L.

6. CONCLUSIONS

A practical constant torque system for a slip ring induction motor using chopper in the rotor circuit has been built and tested. The system is simple, and inexpensive. The torque is easily controlled and can be kept constant over a wide range of speeds.

In the control circuit of the chopper, current settings can be independently adjusted to reduce the motor losses due to harmonics of the rectified current fluctuations. Simple models for the study of system performance at constant torque are presented. The torque slip characteristics show that, the circuit model gives satisfactory results of this current control scheme. Also, the spike in the torque-slip characteristics, and

the harmonics content in the a.c. component of the rectified current decreases as the ratio k is decreased. But in practical controllers, a decrease in k is synonymous with an increase in the switching frequency, resulting in higher switching losses, rating of components increases, and consequently the cost is increased.

A closed loop speed control using chopper in the rotor circuit has also been examined. The system acts to regulate the speed. Also, the difference between the two levels of the rectified current is kept constant and then the harmonic losses due to the rectified current fluctuations are kept approximately constant.

Calculations have been carried out to predict system parameters for acceptable response. The control system stabilizes the speed against load variations using a PI controller . The method of dc dynamic braking resulted in an extremely rapid braking of the drive system. It also eliminates the necessity of a separate d.c. source.

APPENDIX A

Schmitt trigger circuit : The employed Schmitt trigger circuit exhibits a hysteresis loop where the hysteresis voltage is $V_H = V_1 - V_2$. The operational amplifier (LM 324 N) was used as an inverting Schmitt trigger for its high speed and also, it needs only positive voltage power supply. The input voltage (e_i) is applied to the inverting terminal 2 and the reference and the feedback voltages to the noninverting terminal 3, as shown in Figure (A-1). In case of $e_i < V_1$, e_o will be equal to V. Then, using superposition where $R_3 << R_1$ or R_2,

$$V_r = \frac{R_3}{R_2+R_3} V_{ref} + \frac{R_3}{R_1+R_3} V = V_1 \qquad (A-1)$$

Where V_1 is the maximum limit for the value of e_i. If e_i is now increased, then e_o remain constant at V and $V_r = V_1$ = constant until $e_i = V_1$. At this condition the output regeneratively switches to $e_o = 0$ and remains at

this value as long as $e_i > V_r$.

The voltage at the noninverting terminal for $e_o = 0$ is

$$V_r = \frac{R_3}{R_2+R_3} V_{ref} = V_2 \qquad (A-2)$$

Where V_2 is the minimum limit for the value of e_i.

R_1 is chosen such that the loop gain $H_f A_e$ is greater than unity, where $H_f = (R_3)/(R_1+R_3)$ and A_e is the amplifier gain.

Figure (A.2) shows the expected waveforms of the chopper control circuit.

The differentiator : Conventional RC circuits with small time constants are used to differentiate the output of the Schmitt and inverter circuits.

Pulse amplifier : Two transistors are connected as a Derlington-stage to amplify the differentiator output pulses, so that become sufficient for thyristor firing.

APPENDIX B

Motor : Tests have been carried out using a 3-phase, 50 Hz, 4-pole, 1.5 kw, 220 V., slip ring induction motor having the following parameters : $r_1 = 3.09\ \Omega$, $r_2 = 0.196\ \Omega$, $x_1 = 7.09\ \Omega$, $x_2 = 0.2\ \Omega$, $x_m = 180\ \Omega$ and the turns ration N = 5.95. The external rotor resistance $R_x = 28\ \Omega$.

Filter parameters : $L_1 = 230$ m.H. and $R_1 = 2.4\ \Omega$

Control circuit parameters : $R_1 = 100$ k Ω, $R_2 = 10$ K Ω, $R_3 = 120\ \Omega$, $R_4 = 700$ K Ω, $R_5 = 5$ K Ω, $R_6 = 10\ \Omega$ and $C = 0.047\ \mu F$.

Closed loop parameters : $K_1 = 0.024$ V/rad./sec., $R_{sh} = 0.01\Omega$, $F = 1/62$ N.m/rad./sec., $\tau_m = 2$ sec. , $R'_A = 100$ K Ω , $R_B = 1.34\ M\Omega$, and $C_c = 0.2\ \mu F$.

REFERENCES

1] P.C.SEN and K.H.J.MA, "Constant torque operation of induction motors using chopper in rotor circuit", IEEE Trans. IA, Vol. 14, No. 5, pp. 408-414, Sept./Oct. 1978.

2] S.A.MAHMOUD, A.A.ELHEFNAWY, F.GEBRIL and S.A.HASSAN, "Steady-state analysis of chopper-fed d.c. motor", UPEC, Huddersfield, England, 1:3 April 1985.

3] M.RAMAMOORTY and N.S.WANI, "Chopper controlled slip-ring induction motor", IEEE Trans. IECI, Vol. 24, pp. 153-161, May 1977.

4] M.RAMAMOORTY and N.S.WANI, "Dynamic model for a chopper-controlled slip-ring induction motor", IEEE Trans. IECI, Vol. 25, No. 3, pp. 260-266, Aug. 1978.

5] A.E.LASHIN , "Speed control of slip-ring induction motor with chopper in the rotor circuit", M.Sc. thesis, Monoufia University, Egypt, 1985.

6] S.A.MAHMOUD, "DC motor loaded synchronous generator via fully controlled bridge rectifier", UPEC, Sheffield, England, 7:9 April 1981.

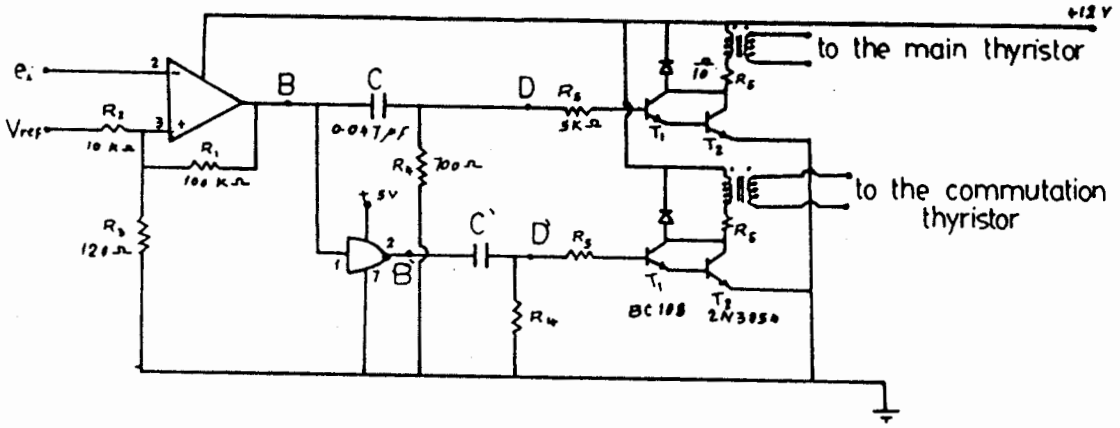

Fig.(A-1) Control circuit of the chopper

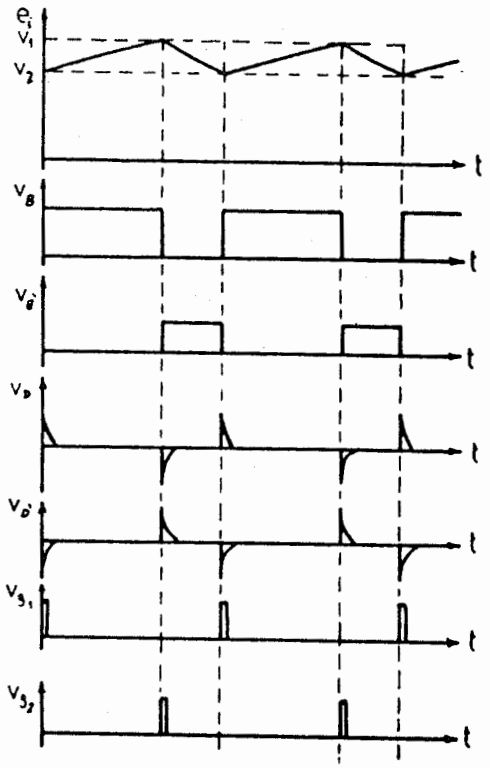

Fig.(A-2) Waveform of the control circuit